



AhR Signaling

Linking diet and immunity

Learn more >>>

InvivoGen



Transcriptional Characterization of the T Cell Population within the Salmonid Interbranchial Lymphoid Tissue

This information is current as of November 15, 2019.

Ida Bergva Aas, Lars Austbø, Melanie König, Mohasina Syed, Knut Falk, Ivar Hordvik and Erling O. Koppang

J Immunol 2014; 193:3463-3469; Prepublished online 29 August 2014;

doi: 10.4049/jimmunol.1400797

<http://www.jimmunol.org/content/193/7/3463>

Supplementary Material <http://www.jimmunol.org/content/suppl/2014/08/28/jimmunol.1400797.DCSupplemental>

References This article **cites 44 articles**, 4 of which you can access for free at: <http://www.jimmunol.org/content/193/7/3463.full#ref-list-1>

Why *The JI*? Submit online.

- **Rapid Reviews! 30 days*** from submission to initial decision
- **No Triage!** Every submission reviewed by practicing scientists
- **Fast Publication!** 4 weeks from acceptance to publication

**average*

Subscription Information about subscribing to *The Journal of Immunology* is online at: <http://jimmunol.org/subscription>

Permissions Submit copyright permission requests at: <http://www.aai.org/About/Publications/JI/copyright.html>

Email Alerts Receive free email-alerts when new articles cite this article. Sign up at: <http://jimmunol.org/alerts>

Errata An erratum has been published regarding this article. Please see [next page](#) or: </content/193/12/6207.full.pdf>

The Journal of Immunology is published twice each month by The American Association of Immunologists, Inc., 1451 Rockville Pike, Suite 650, Rockville, MD 20852
Copyright © 2014 by The American Association of Immunologists, Inc. All rights reserved.
Print ISSN: 0022-1767 Online ISSN: 1550-6606.



Transcriptional Characterization of the T Cell Population within the Salmonid Interbranchial Lymphoid Tissue

Ida Bergva Aas,* Lars Austbø,* Melanie König,*¹ Mohasina Syed,* Knut Falk,[†] Ivar Hordvik,[‡] and Erling O. Koppang*

Previously, our group has shown that the interbranchial lymphoid tissue (ILT) is a distinct structure largely consisting of T cells embedded in a meshwork of epithelial cells, with no direct resemblance to previously described lymphoid tissues. In this study, we aim to focus on the T cell population and the possibility of the ILT being a thymus analog. By characterizing structural responsiveness to Ag challenge, the presence of recombination activating genes, and different T cell–related transcripts, we attempt to further approach the immunological function of the ILT in salmonid gills. In addition to eight healthy individuals, a group of eight infectious salmon anemia virus–challenged fish were included to observe T cell responses related to infection. The results showed reduced size of ILT in the infected group, no expression of RAG-1 and -2, and a high degree of T cell diversity within the ILT. Taking into account that the ILT can be regarded as a strategically located T cell reservoir and possibly an evolutionary forerunner of mammalian MALTs right at the border to the external environment, the alteration in transcription observed may likely represent a shift in the T cell population to optimize local gill defense mechanisms. *The Journal of Immunology*, 2014, 193: 3463–3469.

The gills of fish face a challenging task, combining respiratory function with an exposed position with respect to the external milieu. The mucosal immune system in gills has been addressed in several studies, but only recently a macroscopically detectable lymphoid structure was described, highlighting the significance of gills as a mucosal immune tissue (1, 2). The structure has been named the “interbranchial lymphoid tissue” (ILT) and is located at the terminal portion of the interbranchial gill septa of salmonids (2). It contains predominantly T cells embedded in a meshwork of epithelial cells interconnected by desmosomes (1). Previous investigations have also revealed the presence of MHC class II⁺ cells and some scattered Ig⁺ cells. The

tissue is separated from underlying structures by a prominent basal membrane. Devoid of vessels, it shows no clear resemblance to previously described lymphoid tissues in any species (1–3). The ILT has not yet been designated into the group of primary or secondary lymphoid organs, although transcriptional responses following infection have been observed (4).

Seeing that the thymus and the ILT develop from the same area, it is highly plausible that they share joint functions. The identification of thymus-like lymphoepithelial structures termed thymoids, located in gill tips and secondary lamellae of lamprey larvae (5) has further sparked interest into exciting investigations of lymphoid organizations in gills of teleosts (6).

In teleosts, the primary lymphoid organs are represented by the thymus and the head kidney, where the latter together with the spleen also serves as a secondary lymphoid organ. The thymus is located in the dorsolateral part of the gill chamber and originates from the second to fourth of the pharyngeal pouches (7). Interestingly, the corresponding region also gives rise to the Waldeyer’s ring of secondary lymphoid structures as found in humans (8). The thymus’ main responsibility is T cell maturation, facilitated by a three-dimensional meshwork of epithelial cells creating a lattice-like structure in which immature T cells traffic during the course of their development. A well-founded requirement of primary lymphoid organs is the expression of RAG-1 and RAG-2 genes, and their presence has been used to define tissues responsible for generation of lymphocytes in several teleost species (9–12). Immature T cells are subjected to a RAG-dependent recombination of the TCR genes in the thymus’ cortex and face both positive and negative selection through extensive interaction with epithelial cells (13). Apoptosis, or programmed cell death, plays a crucial role in the strict intrathymic selection of unsuitable T cell candidates (7), and as a consequence, there is considerable apoptotic activity in the thymus (14).

In mammals, an important functional difference between primary and secondary lymphoid organs is their structural responsiveness to antigenic stimuli. Primary lymphoid organs such as thymus and bone marrow, which are concerned with development

*Department of Basic Sciences and Aquatic Medicine, Faculty of Veterinary Medicine and Biosciences, Norwegian University of Life Sciences, 0454 Oslo, Norway; [†]Norwegian Veterinary Institute, 0454 Oslo, Norway; and [‡]Department of Biology, High Technology Centre, University of Bergen, 5006 Bergen, Norway

¹Current address: European Neuroscience Institute, AG Synaptic Vesicle Dynamics, Gottingen, Germany.

Received for publication April 1, 2014. Accepted for publication July 28, 2014.

This work was supported by the Research Council of Norway (InNoVacc project RCN 183196/S40 and FRIMEDBIO-222207/F20).

I.B.A. participated in study design, collection of material, performing the experiments, interpretation of results, statistical analysis, and writing of the manuscript; L.A. managed the study design, the experimental challenge and sampling, primer and probe design, interpretation of results, and writing of the manuscript; M.K. took part in study design, collection of material, and performing the experiments; M.S. took part in planning and design of the study as well as interpretation of results; K.F. designed, participated in execution, and was responsible for the infection experiment and for cultivation of virus; I.H. participated in study design and interpretation of results; E.O.K. supervised the study; and all authors read and approved the manuscript.

Address correspondence and reprint requests to Prof. Erling O. Koppang, Department of Basic Sciences and Aquatic Medicine, Faculty of Veterinary Medicine and Biosciences, Norwegian University of Life Sciences, Ullevålsveien 72, 0454 Oslo, Norway. E-mail address: erling.o.koppang@nmbu.no

The online version of this article contains supplemental material.

Abbreviations used in this article: ct, cycle threshold; IHC, immunohistochemistry; ILT, interbranchial lymphoid tissue; ISAV, infectious salmon anemia virus; MHC I, MHC class I; p.i, postinfection; qPCR, quantitative PCR.

Copyright © 2014 by The American Association of Immunologists, Inc. 0022-1767/14/\$16.00

of lymphocyte effector cells, remain structurally irresponsive when exposed to Ags. In contrast, secondary lymphoid organs involved in maintenance of immune homeostasis and immunoregulation (15) have the capacity to alter their structure to regulate local immune responses. The thymus has a high level of apoptosis because of intrathymic T cell selection. The investigation of structural responsiveness to antigenic stimuli as well as level of apoptosis in the ILT has not been investigated previously. Taken together with the investigation of RAG expression in the ILT, we aim to further characterize the ILT on a functional level to be able to classify it as a primary or secondary lymphoid organ. In addition, the types of T cells present in the ILT were characterized, and the response in control versus infectious salmon anemia virus (ISAV)-challenged fish was measured.

Compared with mammals, characterization of the T cell population in fish has been hampered by limited number of available markers. Not being able to obtain the appropriate array of T cell-related markers, gene expression studies constitute a valuable tool to further elucidate the nature of these cells.

Materials and Methods

Animals and infection protocol

Unvaccinated pre-smolt Atlantic salmon (*Salmo salar*) of Sunndalsøra breed, reared at Nofima, Sunndalsøra, was used for the experiment. The fish hatched in spring 2009 and had an average weight of 574 ± 81 g when sampled. All fish were acclimatized for several weeks and fed until the start of the experiment. No signs of disease were observed prior to ISAV challenge. The uninfected control group and challenged fish were kept in two separate freshwater tanks of 200 l. The water temperature throughout the experiment was $8 \pm 1^\circ\text{C}$. The challenged group was experimentally infected with the ISAV strain Glesvaer by immersion in 50 l freshwater at 7°C with virus at a final concentration of 2×10^4 TCID₅₀ ml⁻¹ for 2.5 h, and subsequently transferred to a new tank (4).

Prior to sampling, fish were anesthetized with 100 mg/ml Finquel MS-222 (Tricain Methanesulfonate). Legal and ethical national requirements and code of practice were implemented in the animal experiments. The experiment was approved by FOTS (Forsøksdyrutvalget til selsyns- og søknadssystem) and conducted in the confined and controlled isolation facilities of the Faculty of Veterinary Medicine and Biosciences, Norwegian University of Life Sciences.

Sampling

The first sampling was performed 9 d postinfection (p.i.) and included six fish from the infected group and four fish from the control group. The second sampling was performed at 27–33 d p.i. and included eight individuals from the infected group and four from the control group. During the sampling procedure, macroscopic examination was performed, and pathological manifestations were registered. Samples were conserved in RNAlater and were collected from the second segment of midintestine (16), hereafter referred to as intestine, midkidney, and gills. In addition, gill samples designated for laser-capture microdissection were snap-frozen in liquid nitrogen for subsequent cryosectioning.

Size measurement of the ILT

Hematoxylin-stained sections from the control group ($n = 8$) and infected group ($n = 8$) were examined using the area estimation of the SL μ Cut microdissection system (Molecular Machines and Industries, Glattburg, Switzerland). In addition to the infected group sampled at 27–33 d p.i., sections from the infected fish sampled at day 9 p.i. ($n = 6$) were included to address the impact of time lapse during infection. Sections from the different groups were randomized to make the measurement unbiased. The size of the ILT was measured by outlining the boundaries of the ILT, excluding the prolongation of the ILT extending upward along the primary lamellae and the epithelial capsule-like layer containing goblet cells. Correlation between area and weight was measured by Pearson's correlation coefficient.

Apoptosis detection by TUNEL

TUNEL staining was performed by using the ApopTag Plus Peroxidase In Situ Apoptosis Detection Kit (Chemicon, Temecula, CA), according to the instructions of the producer, minor adjustments are described. Sections from

all individuals of the control and challenged group (days 27–33) were included. Paraffin sections of 3 μm were cut and mounted on positively charged glass slides (Superfrost plus; Menzel, Braunschweig, Germany) and incubated at 37°C for at least 24 h. Before xylene treatment, tissue sections were incubated at 58°C for 30 min to prevent loosening of tissue sections from glass slides. During color development, the working strength peroxidase substrate was applied and incubated for 3 min at room temperature. Sections were not counterstained. Negative controls (TdT was replaced by equilibration buffer), and positive control slides (provided with the kit) including sections from salmon thymus were included as additional positive controls. Slides were evaluated by light microscopy. Positive staining and morphological signs of apoptosis identified apoptotic cells.

RNA extraction and preparation of cDNA

RNA from whole tissue kept in RNAlater (Qiagen, Hilden, Germany) was isolated using the RNA II kit (Qiagen) following the manufacturers' manual including an integrated DNase step. Concentrations and purity were measured spectrophotometrically with a Biospec-Nano (Shimadzu, Kyoto, Japan) and gel electrophoresis was performed to exclude degradation of RNA. The cDNA synthesis was performed immediately after extraction using Promega Moloney murine leukemia virus reverse transcriptase (Promega, Madison, WI).

For RNA sampling from laser-captured tissue, transversal cryosections of the gill primary lamellae, 10 μm in thickness, were cut using a cryostat (Leitz Cryostat 1720; Leitz, Wetzlar, Germany) and mounted on special membrane slides (Molecular Machines and Industries, Zurich-Glattburg, Switzerland). The sections were air-dried for 1 h at room temperature and stained with RNase-free hematoxylin stain and air dried for 30 min. Slides were kept in an exsiccation chamber until laser capture microdissection. The ILTs were dissected, excluding the epithelial capsule-like layer (Fig. 1A, 1B). To ensure that the material was representative and sufficient, several ILTs from parallel sections were microdissected to obtain an area corresponding to $1\text{--}2 \times 10^6 \mu\text{m}^2$ or $\sim 7\text{--}10$ parallel ILTs from each fish and collected in separate tubes (Molecular Machines and Industries).

RNA from laser-captured tissue was isolated using the NucleoSpin RNA XS (Macherey and Nagel, Duren, Germany) following the manufacturer's manual including an integrated DNase step. The RNA was eluted in 15 μl RNase free H₂O and directly used for cDNA synthesis.

As expected, RNA yield from laser-dissected ILT was too low to measure quantitatively; this cDNA was prepared using the total RNA eluate and Moloney murine leukemia virus reverse transcriptase (Promega). The cDNA synthesis was prepared with oligo(dT) and random hexamer primers and RNase to prevent any RNA degradation.

Quantitative real-time PCR

Real-time quantitative PCR (qPCR) was performed using TaqMan Gene Expression Master Mix (Applied Biosystems, Foster City, CA) and carried out in a 7900HT fast real-time PCR system (Applied Biosystems). Primers and probes were designed to span intron sections. To exclude any sequence polymorphism that could interfere with binding of primers and probe, all available salmonid sequences (annotated, expressed sequence tags, salmon genome, and RNaseq) were taken into account. The primer and probe sequences for EF1A_B, CD3 ζ , TCR α , TCR δ , CD4-1, CD4-2a, CD4-2b, CD8 α , CD8 β , MHC class I (MHC I), MHC II, RAG-1, and RAG-2 transcripts are listed in Table I. The expression level was measured with relative quantification using elongation factor 1A EF1A_B (17, 18) as a reference gene, and gene expression was calculated from cycle threshold (Ct) values using the $\Delta\Delta\text{Ct}$ method (19). Real-time qPCR was carried out

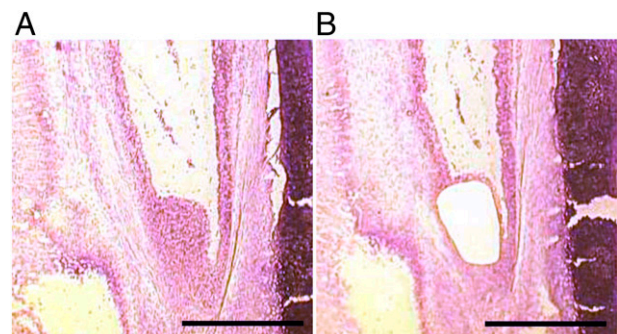


FIGURE 1. Laser-capture microdissection of ILT. Micrographs of a cryosection before (**A**) and after (**B**) laser-capture microdissection of ILT. Hematoxylin counterstain. Scale bar, 50 μm .

Table I. Gene assays used for quantitative real-time RT-PCR

| Gene | Gene Sequence (5'→3') | GenBank Accession No. |
|---------------------|----------------------------------------------------------------------------------------------|-----------------------|
| EF1A _B * | F-TGCCCTCCAGGATGTCTAC R-CACGGCCCACAGGTACTG P-FAM-AAATCGGCGGTATTGG-MGB | BG933853 |
| CD3 ζ | F-AACAGGGATCCAGAGAGTGTCTG R-AAGGGACGTGTAAGTGTCTCA P-FAM-ACGGCACCGGATAATCGCAGGA-BHQ | BT060238.1 |
| TCR α | F-AACTGGTATTTTGACACAGATGC R-ATCAGCACGTGAAAACGAT P-FAM-ACCATTTCTGGCCTGAGAATTCTGT-BHQ | AY552002 |
| TCR δ | F-AGCGTTGTGAGATGGATGGC R-GCAGTTGTAGCCGTGGTGTATAG P-FAM-AGCCGCCGTTGATGATAAAGATGATTC-BHQ | EF467299 |
| CD4-2a | F-GCCCCGAAGTCCAACGAC R-AGGCTTCTCTCACTGCGTCC P-FAM-CCGCACACTAGAGGGTCCACCACG-BHQ | EU409792 EU409793 |
| CD4-2b | F-TACTGCCAGTGTAAACCGCAC R-GTGTCTGTCGATCAAGGATGT P-ACAGCGCTGATGGAGCGGAGTATTA-BHQ | CA060137 |
| CD4-1 | F-TCTGCCGCTGCAAAGACC R-GCCAAGACGAAATAGTAGAGACA P-ATCATACAGACCCGGAATCCCTGTCA-BHQ | EU409794 |
| CD8 α | F-ACTTGCTGGGCCAGCC R-CACGACTTGGCAGTTGTAGA P-CGACAACAACAACCACCACG-BHQ | NM_001123583 |
| CD8 β | F-TTCTTCTCAGACCCGGAGAA r-ATCGTTCCTTTTGGTGCAG p-CAACATTAACCCCTGTCACGAAGC-BHQ | AY693394 |
| MHC I | F-GGAAGAGCACTCTGATGAGGACAG R-CACCATGACTCCACTGGGGTAG P-TCAGTGCTCTGCTCCAGAAGACCCCT-BHQ | JN561337 |
| MHC II | F-CCACCTGGAGTACACCCAG R-TTCCTCTCAGCCTCAGGCAG P-FAM-TCCTGCATGGTGGAGCACATCAGC-BHQ | X70165 |
| RAG-1 | F-GAGGCCATGATGCAAGGC R-CTTGACGGTGCAGTACATCT P-FAM-ATCCTGCTGTGTCTGGCCATC-BHQ | NM_001124737 |
| RAG-2 | F-GTTCCTCGAGACGTTCAAAACAG R-TTCACTGCAGTCAAGTGTG P-FAM-ACGTTAGCTACTTGAGCAGGAGCCAC-BHQ | DY697789 U25146 |

Gene assays used for quantitative real-time RT-PCR with relevant accession numbers (National Center for Biotechnology Information database; <http://www.ncbi.nlm.nih.gov/>). Primers and probes are designed to span intron sections. Asterisk (*) indicates assays designed by others, EF1A_B (17).

in 13 μ l reactions with the following uniform temperature profile: 10 min at 95°C, 40 cycles of 15 s at 95°C, 15 s at 58°C, and 60 s at 60°C (45 cycles for the laser-dissected samples). Template or cDNA corresponding to 15 ng RNA were added in each reaction. To compensate for lower template concentration, the laser-dissected cDNA samples were diluted 5 times instead of 10. Each quantification target was amplified in triplicate samples (whole tissue) or duplicate samples (laser-dissected tissue) with additional negative controls, lacking the template, for each master mix. The data were analyzed using Sequence Detection Systems Software version 2.3 (Applied Biosystems). Statistical differences in gene expression in control and infected tissue samples were evaluated using the nonpaired *t* test. Differences in expression between the control and challenged group were considered to be significant with *p* values < 0.05 ($\alpha = 0.05$). In addition, Bonferroni correction was performed to account for multiple tests, using the formula $\alpha/\text{number of tests performed}$. All analyses were performed using GraphPad Prism version 6 for Windows (GraphPad Software, San Diego, CA; <http://www.graphpad.com>).

Results

Gross pathology/infection status

The first sampling was performed at day 9 p.i. The second sampling was conducted at days 27–33 p.i., when the fish were in a terminal stage of disease, confirmed by mortality starting at day 33 p.i. Pathological examinations at the last sampling revealed classical findings including swollen liver and spleen, which also were dark and enlarged. Petechial bleedings in the eyes, fins, and peritoneal organs were recorded in addition to ascites and anemia.

Total ISAV was measured using real-time qPCR and a TaqMan assay designed against ISAV segment 8 for diagnostic purposes (20). Increasing levels of virus in midkidney and gill of infected fish sampled on day 9 and onward confirmed the bath challenge to be successful. The transcriptional response of innate immune genes and ISAV were comparable to that observed by Austbø et al. (4) and were observed in all individuals (data not shown). Their upregulation indicates a strong systemic response, in line with the increased virus levels that were measured in all the individuals investigated.

Size of the ILT

A 20% (19.92) decrease in size of the ILT compared with the control group was observed at the first sampling performed 9 d p.i., and a 34% (34.15) decrease at the second sampling performed at 27–33 d p.i. To exclude the possibility that the size of the fish would affect these measurements, we confirmed that there was no significant correlation between size of the ILT and the weight of the fish (Supplemental Table I) ($r = 0.23$, $p = 0.30$).

Apoptosis in the ILT

A negligible number of apoptotic cells were identified within the ILT, and there were no significant difference between the number of apoptotic cells within the ILT in the control fish (Fig. 2A) compared with infected individuals (Fig. 2B). Positive controls provided

with the kit were confirmed, and apoptotic cells were identified in salmon thymus sections (Fig. 2C).

Presence of RAG-1 and RAG-2 transcripts

RAG-1 and RAG-2 transcripts (Fig. 3) were investigated in ILT, gill, intestine, and midkidney from the control and challenged group in addition to thymic tissue from the control group as a positive control. Transcripts corresponding to RAG-1 and RAG-2 were found in the thymus and midkidney. In the gills, RAG-1 transcripts were present in 12 of 16 fish examined, whereas transcripts corresponding to RAG-2 were present in all 16 fish. In intestine, only transcripts corresponding to RAG-2 were present. Transcripts corresponding to RAG-1 and RAG-2 were absent in the ILT.

Transcription of T cell-related markers

Real-time qPCR analysis was performed on laser-dissected ILT in addition to samples from gill, midkidney and intestine from eight control individuals and eight from the challenged group sampled on days 27–33 p.i.

The real-time qPCR showed a relatively low variance between the triplicates and within the groups. For the laser-dissected ILT samples, the expected RNA yield is too low to measure quantitatively. To ensure the presence of sufficient template in the laser-dissected samples, a Ct threshold of 28 was set for the reference gene EF1A_B. Samples exceeding this Ct were harvested and isolated again so that all analyzed samples were below this threshold. To ensure that laser capture microdissection did not interfere with transcript integrity, test samples from gills (one infected and one uninfected) were harvested using laser capture microdissection and run on all TaqMan assays. The results showed minimal differences between whole gill sampled by laser capture microdissection and from tissue embedded in RNAlater.

The expression level in the healthy population showed that all T cell-related transcripts investigated were present in all organs examined (Fig. 4). A majority of the transcripts investigated were expressed highest in the ILT, except, for example, MHC I and MHC II, which were most prominent in the mucosal tissues, gills, and intestine. Individual transcript levels for the T cell-related markers including significant alterations in transcript levels are presented in Fig. 5, which also shows significance after application of Bonferroni correction. All mean Ct values \pm SEM are given in Supplemental Table II.

In the control group, the pan T cell marker CD3 showed a 1.7-fold higher transcript level in the ILT compared with control gills (Fig. 5). The lowest level was found in intestine (0.3-fold). An increased level of CD3 ζ transcripts was observed in ILT of the infected population. In the gill, the transcript level remained relatively stable, whereas in intestine and midkidney, the increase was significant.

Relative to EF1A_B, TCR α and TCR δ transcript level was the highest in ILT compared with the other tissues examined. A significant decrease of TCR α transcript level but not for TCR δ was observed in the ILT of the infected population. The TCR α/δ ratios (Supplemental Table III) in the control and infected group displayed differences between the tissues. Following infection, the ratio decreased in the ILT (control: 7.7, infected 4.2) and midkidney (control: 8.4, infected: 6.6), increased in the gill (control: 9.2, infected: 12), and remained stable in the intestine (control: 27.4, infected: 27.8).

Independent of group and tissue, the transcript level of CD4-2a was the highest compared with CD4-2b and CD4-1. Relative to EF1A_B, the CD4-2a and CD4-2b transcript level was highest in the ILT and for all CD4 transcripts lowest in intestine of the control group. In the gills, intestine, and midkidney, a significant increase of CD4-2a transcripts was observed in the challenged fish.

CD8 α/β transcripts were present in the ILT, gill, intestine, and midkidney. Relative to EF1A_B, the transcript level of CD8 α and CD8 β in the healthy population was higher in the ILT compared with the other tissues and remained nearly unaffected in the infected group. The CD8 α/β ratio showed significant differences between the tissues (Supplemental Table III). The highest CD8 α/β ratio was found in the ILT (control = 1.0, infected = 1.1), and the ratios remain relatively stable in the infected population.

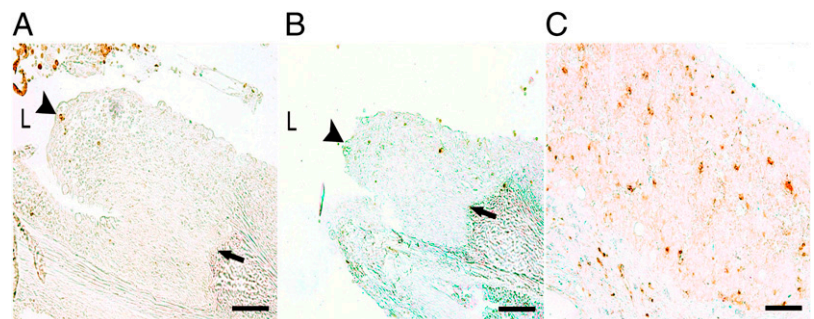
The transcript level of MHC I in the control group was highest in gill (Ct = 16.9 \pm 0.5) and intestine (Ct = 17.7 \pm 0.6), markedly lower in the ILT (Ct = 24.8 \pm 3) and midkidney (Ct = 21 \pm 1.2). In the infected group, an increase in MHC I transcripts was observed across all tissues, with significant changes observed in gill, intestine, and midkidney.

The MHC II transcript level was highest in gill (Ct = 18.7 \pm 0.4) and intestine (Ct = 20.7 \pm 0.9) compared with ILT (Ct = 26.2 \pm 3.5) and midkidney (Ct = 23.5 \pm 1.3) in the healthy individuals. No response was detected in the infected population.

Discussion

From previous studies using immunohistochemistry (IHC), it has been stated that the ILT is a defined tissue predominantly consisting of CD3⁺ T cells embedded in a lattice-like system of epithelial cells. The only other known tissue having such an organization of T cells and epithelial cells is the thymus. Therefore, and together with the fact that these two tissues are located in close proximity to each other and develop from the same area, it is likely to presume that the ILT could have evolved from or possess analog functions to the thymus. In this study, we aimed at uncovering the function of the ILT by using different approaches. By investigating the ILTs structural responsiveness to antigenic stimuli, the level of apoptosis as well as expression of RAG genes, we were able to further elucidate functional aspects of the ILT that would help us in further characterizing it as a primary or secondary lymphoid

FIGURE 2. Apoptosis detection by TUNEL. Negligible number of apoptotic cells detected in ILT from control (A) and infected fish (B), compared with salmon thymus (C) as a positive control. Apoptotic cells stain brown. No counterstain. Arrow, basal membrane of ILT; arrowhead, surface of ILT; L, branchial chamber. Scale bar, 10 μ m.



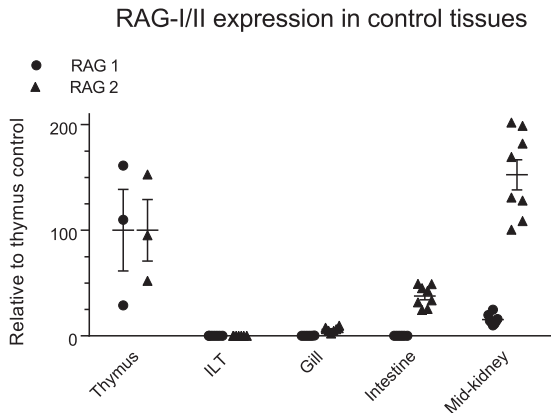


FIGURE 3. Detection of RAG-1 and RAG-2 transcripts in thymus, laser-dissected ILT, gill, intestine, and midkidney. RAG-1 and RAG-2 transcripts quantified by real-time qPCR in control ($n = 8$) salmon. The individual transcript level for each fish is displayed with mean (\pm SEM) set to 100. Transcript levels are normalized with EF1A_B and displayed relative to the mean of thymus control ($n = 3$).

organ. In addition, we have characterized the T cell population present, and its response in infected fish.

An interesting observation in the ISAV-infected fish was a decrease in size of the ILT compared with the healthy fish.

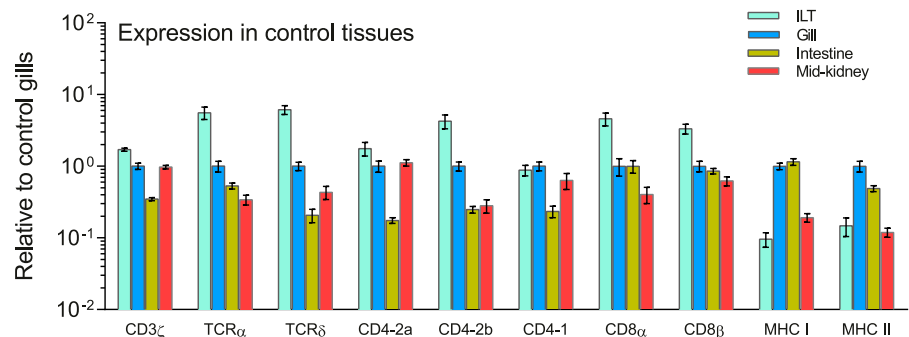
Succeeding randomized investigations of ILT's size in two infected groups at different time points (days 9 and 27–33 p.i.) confirmed the decrease to be significant. To exclude the possibility of apoptosis being the cause of size reduction, TUNEL staining was performed and revealed that the number of apoptotic cells within the ILT was not significantly different in the control and infected population. In sharp contrast, considerable apoptotic activity was found in the thymus. Whether the decrease in size is a consequence of T cell migration from the ILT to other locations exposed to Ags or shrinkage of the organ due to infection remains unknown, but future studies will be designed to focus on these questions.

In mammals, it has been shown that in the primary lymphoid organs (thymus and bone marrow), the RAG-dependent V(D)J recombination of T and BCR genes takes place, and are therefore considered as a developmental marker of primary lymphoid organs (9). In our study, transcripts corresponding to RAG-1 and RAG-2 were confirmed in the thymus. However, in the ILT, transcripts of both RAG variants were absent in the control and infected group, ruling out the possibility of the ILT being a true equivalent to the thymus. Taking into consideration the additional genome duplication in salmonids, available sequence databases have been browsed (using blastn, blastx, and tblastx) without finding any additional sequences that could be identified as RAG genes. However, based on the age and size of the examined fish, we cannot rule out that RAG expression and consequently the func-

tion of ILT could be different during earlier developmental stages. In line with previous studies, RAG-1 and RAG-2 transcripts were present in midkidney as previously shown in carp (*Cyprinus carpio*) (21), and in rainbow trout (*Oncorhynchus mykiss*) (only RAG-1), in gills and intestine with a very low or undetectable level of RAG-1 (9).

As in mammals, the teleost TCR is found on the surface of mature T cells present as two subpopulations, TCR $\alpha\beta$ - and $\gamma\delta$ (22), with several important differences in both distribution and function. Their orthologs have been characterized in salmon (23, 24). In vertebrates, the $\alpha\beta^+$ T cells reside mainly in secondary lymphoid organs and constitute most mature T cells (25). In mammals, $\gamma\delta^+$ T cells constitute a small population known as intraepithelial lymphocytes, most abundant in the skin, gut, lung, and tongue. Residing in the epithelial layers of mucosal tissues (25), they have been reported to respond rapidly to tissue stress by release of cytokines, giving these cells a key role in immune regulation (26). In addition to confirming the presence of TCR α - and δ transcripts in the ILT, we showed that their relative transcript levels were higher in the ILT compared with gill, mid-kidney, and intestine. The presence of TCR δ transcripts in the ILT underlines the importance of $\gamma\delta^+$ T cells in mucosal surfaces as previously shown in sea bass (*Dicentrarchus labrax*) (27). The TCR α transcript level in the ILT was significantly decreased following infection, representing a reaction pattern different from that observed in gill, midkidney, and intestine, where no significant changes were observed. This finding demonstrated that the ILT responded to systemic infection in a distinct manner compared with the other tissues examined, especially noteworthy the gills, in which the ILT is embedded. Previous investigations have shown the presence of the ISAV cellular receptor in the ILT by IHC (28), whereas the absence of replicating ISAV has been shown by a RT-qPCR assay (4). These findings indicate that the changes observed in the ILT most likely are consequences of a systemic and not a local response. Once we compared the TCR α /TCR δ ratio in the ILT and gill, it was evident that the ILT not only has the highest transcript levels of TCR α and TCR δ but also the lowest TCR α /TCR δ ratio. In the challenged fish, the ratio decreased dramatically (control: 7.7, infected: 4.2). The same trend was present in the midkidney, a primary/secondary lymphoid organ (control: 8.4, infected: 6.6). In sharp contrast, a simultaneous increase of the TCR α /TCR δ ratio in the gill could be observed (control: 9.2, infected: 12). The ratio in the intestine remained relatively unaffected (control: 27.4, infected: 27.8). The altered ratios might be the result of redistribution of $\alpha\beta^+$ / $\gamma\delta^+$ T cells by migration into or out of the tissue. Nevertheless, it might be interpreted as an attempt to optimize local defense mechanisms. A rapid redistribution of $\gamma\delta^+$ T cells from mucosal sites to lymphoid sites was observed in macaques (*Macaca mulatta*) following oral infection of SIV (29). In sea bass (*Dicentrarchus labrax*), the same observations have been made

FIGURE 4. T cell-related transcript levels in the control group. Analysis of T cell-related markers show that all transcripts investigated were present in all organs examined. Transcript levels for the control group ($n = 8$) are displayed with mean \pm SEM. Transcript levels are normalized with EF1A_B and displayed relative to the mean of control gills.



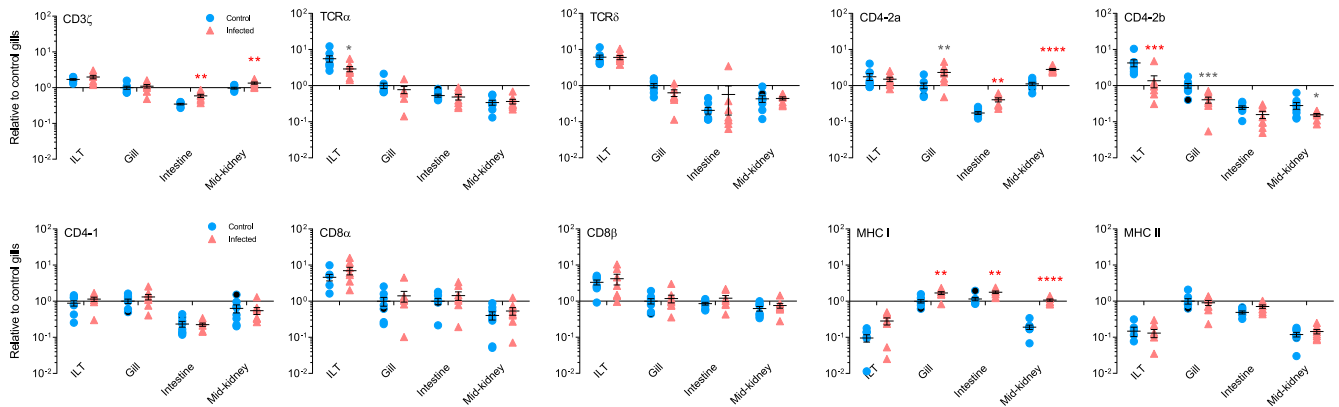


FIGURE 5. T cell-related transcripts in control and ISAV-infected salmon. Analysis of T cell-related transcripts in laser-dissected ILT, gill, intestine, and midkidney of control ($n = 8$) and ISAV-infected salmon ($n = 8$) quantified by real-time qPCR. Significant changes in transcription level by days 27–33 p.i.; $****p < 0.0001$, $***p < 0.001$, $**p < 0.01$, $*p < 0.05$. Stars colored red indicates significance at $p < 0.005$, according to Bonferroni correction, performed to account for multiple tests. The individual transcript level for each fish is displayed with mean \pm SEM. Transcript levels are normalized with EF1A_B and displayed relative to the mean of control gills.

following viral infection, indicating that $\gamma\delta^+$ T cells have a role in virus-induced immunity also in teleosts (25).

The CD3 complex is considered to be a pan T cell marker, and the CD3 orthologs have been characterized in salmon (30). In accordance with former IHC results (1, 2), our study showed high levels of CD3 ζ transcripts in the ILT compared with the other tissues examined. In the infected group, a moderate increase of the CD3 ζ transcript level was observed in all tissues examined but only significant in the intestine and midkidney. This is not necessarily caused by an upregulation of CD3 expression but more likely a possible mobilization of a T cell-mediated immune response.

In teleosts, T cells are further divided into T helper cells displaying a CD4 coreceptor and cytotoxic T cells displaying a CD8 coreceptor (31). Th cells interact with MHC II, recognizing exogenous Ag. In contrast, cytotoxic T cells interact with MHC I and recognize endogenous Ag (32). In contrast, expression of CD4 and CD8 are absent from most $\gamma\delta^+$ T cells (33). Orthologs of both CD4 and CD8 have been identified in salmonids (34–36) with certain structural differences. Transcripts corresponding to the three CD4 variants were identified in all tissues examined; CD4-2a was the variant with the highest transcript level in all tissues examined, a finding that corresponds with previous observations examining the expression of different CD4 variants in Atlantic salmon (35). In the infected population, a significant increase in CD4-2a transcripts was observed in the gills, midkidney, and intestine but not in the ILT.

The CD8 coreceptor is commonly represented by a heterodimer consisting of a CD8 α and CD8 β subunit, encoded by two distinct genes (37). A less common CD8 $\alpha\alpha$ homodimer can be found on subsets of intraepithelial lymphocytes, both $\alpha\beta^+$ and $\gamma\delta^+$ T cells, mast cells, macrophages, NK cells and subsets of dendritic cells (38). In our study, the transcript levels of CD8 α and CD8 β were higher in the ILT compared with the other tissues examined. This observation correlates with previous studies on distribution of CD8 $^+$ cells in rainbow trout (*Onchorhynchus mykiss*), showing an accumulation of CD8 α^+ cells in the ILT, gill and intestine (39). Interestingly, the CD8 α /CD8 β ratio in the ILT (control: 1.0, infected: 1.1) was significantly higher than in gill (control: 0.6, infected: 0.6), intestine (control: 0.7, infected: 0.7) and midkidney (control: 0.4, infected: 0.4), and remained stable in the infected population. This finding indicated that the proportion of CD8 α^+ cells is higher in the ILT, and might be explained by the presence of CD8 $\alpha\alpha$ homodimers, which are known for their repressor effect on T cell activation, acting by decreasing the functional avidity between the TCR–MHC complex (40). The presence of CD8 α^+

NK cells, equivalent to the CD8 α^+ NK cells of humans, has been suggested in rainbow trout (40).

The transcript level of MHC I increased in all tissues in the infected population. In gill, intestine, and midkidney, the increase was significant. These findings correlated with previous investigations in ISAV-infected Atlantic salmon (41, 42) and can be seen in the context of a T cell-mediated immune response as a consequence of infection.

MHC II is also present in the ILT (41) but at a considerably lower transcript level compared with MHC I. Consistent with previous publications (41, 43), both MHC I and II showed highest expression in gills and intestine, which may be a reflection of their alerted state because of a high Ag exposure. Compared with MHC I, MHC II had a relatively stable transcript level that was maintained throughout the sampling period and was unaffected by infection.

This study has by multiple approaches examined responses of the ILT to infection and has by far excluded the possibility that this tissue is a primary lymphoid organ at least during the investigated developmental stage. An important hallmark of primary lymphoid organs is their structural irresponsiveness to antigenic stimuli (5) and expression of RAG genes to allow recombination of T and BCR genes to take place (44, 45). The fact that the ILT is not a static structure but is responsive to antigenic stimuli and the absence of RAG transcripts further indicates that the ILT most likely is a secondary lymphoid organ. On the basis of the present alteration in transcript levels and a strong positive correlation for TCR α /CD42a (data not included), one may speculate that it is TCR $\alpha\beta^+$ cells, possibly CD4 $^+$ cells that migrate from the ILT out in the gill filament, most likely to communicate with APCs. In addition, we have shown that the ILT is composed of a highly heterogeneous group of T cells. The ILT expresses several markers for the adaptive arm of the immune system, which might indicate that the structure is an important site for the induction of local T cell-mediated immunity. The ILT responds to infection in a different manner compared with the other tissues examined, especially noteworthy the gills, in which the ILT is located. The gills as a mucosal tissue have previously been hypothesized as the location of less evolved lymphoid organizations in teleosts (6). The strategic location of the ILT gives the mucosal immune system a unique possibility of an early onset of local immune mechanisms right at the border to the external environment, a location that under no doubt is subjected to considerable exposure of both unharmed commensal microorganisms and Ags presenting a threat to the organism. The presence of peaceful coexistence

with commensals depends on mechanisms that limit the initiation of immune responses unless strictly required, similar to that found in lungs of humans (46). Similarly, clonal anergy of B cells might represent another surveillance system in the gills (6). The extraordinary heterogeneous population of T cells located within the ILT contributes beyond doubt to the local immune defense in the gills, and future studies will aim to reveal the mechanisms by which the ILT exerts its function.

We conclude that the ILT most likely is a secondary lymphoid structure; however, it lacks key features of organized MALT as seen in mammals such as vessels and germinal centra. With its location in the pharyngeal region, this opens up for the possibility that the ILT represents nature's early attempt to develop organized MALT.

Acknowledgments

We thank Emil Westad and Alf Seljenes Dalum (Faculty of Veterinary Medicine and Biosciences, Norwegian University of Life Sciences) for assistance during sampling and for assistance with photo editing, respectively, Simon Chioma Weli (Norwegian Veterinary Institute) for cultivation of virus, and Bjørn Møller (Cancer Registry of Norway, Oslo, Norway) for statistical assistance.

Disclosures

The authors have no financial conflicts of interest.

References

- Haugravoll, E., I. Bjerkås, B. F. Nowak, I. Hordvik, and E. O. Koppang. 2008. Identification and characterization of a novel intraepithelial lymphoid tissue in the gills of Atlantic salmon. *J. Anat.* 213: 202–209.
- Koppang, E. O., U. Fischer, L. Moore, M. A. Tranulis, J. M. Dijkstra, B. Köllner, L. Aune, E. Jirillo, and I. Hordvik. 2010. Salmonid T cells assemble in the thymus, spleen and in novel interbranchial lymphoid tissue. *J. Anat.* 217: 728–739.
- Aamelfot, M., S. C. Weli, O. B. Dale, E. O. Koppang, and K. Falk. 2013. Characterisation of a monoclonal antibody detecting Atlantic salmon endothelial and red blood cells, and its association with the infectious salmon anaemia virus cell receptor. *J. Anat.* 222: 547–557.
- Austbø, L., I. B. Aas, M. König, S. C. Weli, M. Syed, K. Falk, and E. O. Koppang. 2014. Transcriptional response of immune genes in gills and the interbranchial lymphoid tissue of Atlantic salmon challenged with infectious salmon anaemia virus. *Dev. Comp. Immunol.* 45: 107–114.
- Bajoghli, B., P. Guo, N. Aghaalaie, M. Hirano, C. Strohmaier, N. McCurley, D. E. Bockman, M. Schorpp, M. D. Cooper, and T. Boehm. 2011. A thymus candidate in lampreys. *Nature* 470: 90–94.
- Castro, R., E. Bromage, B. Abós, J. Pignatelli, A. González Granja, A. Luque, and C. Tafalla. 2014. CCR7 is mainly expressed in teleost gills, where it defines an IgD⁺IgM⁺ B lymphocyte subset. *J. Immunol.* 192: 1257–1266.
- Bowden, T. J., P. Cook, and J. H. W. M. Rombout. 2005. Development and function of the thymus in teleosts. *Fish Shellfish Immunol.* 19: 413–427.
- Matsunaga, T., and A. Rahman. 2001. In search of the origin of the thymus: the thymus and GALT may be evolutionarily related. *Scand. J. Immunol.* 53: 1–6.
- Hansen, J. D., and S. L. Kaattari. 1995. The recombination activation gene 1 (RAG1) of rainbow trout (*Oncorhynchus mykiss*): cloning, expression, and phylogenetic analysis. *Immunogenetics* 42: 188–195.
- Hansen, J. D., and S. L. Kaattari. 1996. The recombination activating gene 2 (RAG2) of the rainbow trout *Oncorhynchus mykiss*. *Immunogenetics* 44: 203–211.
- Danilova, N., V. S. Hohman, F. Sacher, T. Ota, C. E. Willett, and L. A. Steiner. 2004. T cells and the thymus in developing zebrafish. *Dev. Comp. Immunol.* 28: 755–767.
- Zwollo, P., S. Cole, E. Bromage, and S. Kaattari. 2005. B cell heterogeneity in the teleost kidney: evidence for a maturation gradient from anterior to posterior kidney. *J. Immunol.* 174: 6608–6616.
- Romano, N., A. J. Taverne-Thiele, M. Fanelli, M. R. Baldassini, L. Abelli, L. Mastroli, W. B. Van Muiswinkel, and J. H. Rombout. 1999. Ontogeny of the thymus in a teleost fish, *Cyprinus carpio L.*: developing thymocytes in the epithelial microenvironment. *Dev. Comp. Immunol.* 23: 123–137.
- Romano, N., G. Ceccarelli, C. Caprera, E. Caccia, M. R. Baldassini, and G. Marino. 2013. Apoptosis in thymus of teleost fish. *Fish Shellfish Immunol.* 35: 589–594.
- Boehm, T., and C. C. Bleul. 2007. The evolutionary history of lymphoid organs. *Nat. Immunol.* 8: 131–135.
- Løkka, G., L. Austbø, K. Falk, I. Bjerkås, and E. O. Koppang. 2013. Intestinal morphology of the wild Atlantic salmon (*Salmo salar*). *J. Morphol.* 274: 859–876.
- Olsvik, P. A., K. K. Lie, A.-E. O. Jordal, T. O. Nilsen, and I. Hordvik. 2005. Evaluation of potential reference genes in real-time RT-PCR studies of Atlantic salmon. *BMC Mol. Biol.* 6: 21.
- Løvoll, M., L. Austbø, J. B. Jørgensen, E. Rimstad, and P. Frost. 2011. Transcription of reference genes used for quantitative RT-PCR in Atlantic salmon is affected by viral infection. *Vet. Res.* 42: 8.
- Schmittgen, T. D., and K. J. Livak. 2008. Analyzing real-time PCR data by the comparative C(T) method. *Nat. Protoc.* 3: 1101–1108.
- Snow, M., P. McKay, A. J. McBeath, J. Black, F. Doig, R. Kerr, C. O. Cunningham, A. Nylund, and M. Devold. 2006. Development, application and validation of a Taqman real-time RT-PCR assay for the detection of infectious salmon anaemia virus (ISAV) in Atlantic salmon (*Salmo salar*). *Dev. Biol.* 126: 133–145; discussion 325–326.
- Huttenhuis, H. B. T., M. O. Huisling, T. van der Meulen, C. N. van Oosterhoud, N. A. Sánchez, A. J. Taverne-Thiele, H. W. J. Stroband, and J. H. W. M. Rombout. 2005. Rag expression identifies B and T cell lymphopoietic tissues during the development of common carp (*Cyprinus carpio*). *Dev. Comp. Immunol.* 29: 1033–1047.
- Laing, K. J., and J. D. Hansen. 2011. Fish T cells: recent advances through genomics. *Dev. Comp. Immunol.* 35: 1282–1295.
- Hordvik, I., J. Torvund, L. Moore, and C. Endresen. 2004. Structure and organization of the T cell receptor α chain genes in Atlantic salmon. *Mol. Immunol.* 41: 553–559.
- Yazawa, R., G. A. Cooper, M. Beetz-Sargent, A. Robb, L. McKinnel, W. S. Davidson, and B. F. Koop. 2008. Functional adaptive diversity of the Atlantic salmon T-cell receptor γ locus. *Mol. Immunol.* 45: 2150–2157.
- Buonocore, F., R. Castro, E. Randelli, M.-P. Lefranc, A. Six, H. Kuhl, R. Reinhardt, A. Facchiano, P. Boudinot, and G. Scapigliati. 2012. Diversity, molecular characterization and expression of T cell receptor γ in a teleost fish, the sea bass (*Dicentrarchus labrax*, L.). *PLoS One* 7: e47957.
- Bonneville, M., R. L. O'Brien, and W. K. Born. 2010. $\gamma\delta$ T cell effector functions: a blend of innate programming and acquired plasticity. *Nat. Rev. Immunol.* 10: 467–478.
- Boschi, I., E. Randelli, F. Buonocore, D. Casani, C. Bernini, A. M. Fausto, and G. Scapigliati. 2011. Transcription of T cell-related genes in teleost fish, and the European sea bass (*Dicentrarchus labrax*) as a model. *Fish Shellfish Immunol.* 31: 655–662.
- Aamelfot, M., O. B. Dale, S. C. Weli, E. O. Koppang, and K. Falk. 2012. Expression of the infectious salmon anaemia virus receptor on Atlantic salmon endothelial cells correlates with the cell tropism of the virus. *J. Virol.* 86: 10571–10578.
- Kosub, D. A., A. Durudas, G. Lehrman, J. M. Milush, C. A. Cano, M. K. Jain, and D. L. Sodora. 2008. Gamma/Delta T cell mRNA levels decrease at mucosal sites and increase at lymphoid sites following an oral SIV infection of macaques. *Curr. HIV Res.* 6: 520–530.
- Liu, Y., L. Moore, E. O. Koppang, and I. Hordvik. 2008. Characterization of the CD3 ζ , CD3 $\gamma\delta$ and CD3 ϵ subunits of the T cell receptor complex in Atlantic salmon. *Dev. Comp. Immunol.* 32: 26–35.
- Castro, R., D. Bernard, M. P. Lefranc, A. Six, A. Benmansour, and P. Boudinot. 2011. T cell diversity and TcR repertoires in teleost fish. *Fish Shellfish Immunol.* 31: 644–654.
- Nakanishi, T., H. Toda, Y. Shibasaki, and T. Somamoto. 2011. Cytotoxic T cells in teleost fish. *Dev. Comp. Immunol.* 35: 1317–1323.
- Hayday, A. C. 2000. $\gamma\delta$ cells: a right time and a right place for a conserved third way of protection. *Annu. Rev. Immunol.* 18: 975–1026.
- Moore, L. J., T. Somamoto, K. K. Lie, J. M. Dijkstra, and I. Hordvik. 2005. Characterisation of salmon and trout CD8 α and CD8 β . *Mol. Immunol.* 42: 1225–1234.
- Moore, L. J., J. M. Dijkstra, E. O. Koppang, and I. Hordvik. 2009. CD4 homologues in Atlantic salmon. *Fish Shellfish Immunol.* 26: 10–18.
- Fischer, U., E. O. Koppang, and T. Nakanishi. 2013. Teleost T and NK cell immunity. *Fish Shellfish Immunol.* 35: 197–206.
- Littman, D. R., Y. Thomas, P. J. Maddon, L. Chess, and R. Axel. 1985. The isolation and sequence of the gene encoding T8: a molecule defining functional classes of T lymphocytes. *Cell* 40: 237–246.
- Cheroutre, H., and F. Lambolez. 2008. Doubting the TCR coreceptor function of CD8 α . *Immunity* 28: 149–159.
- Takizawa, F., E. O. Koppang, M. Ohtani, T. Nakanishi, K. Hashimoto, U. Fischer, and J. M. Dijkstra. 2011. Constitutive high expression of interleukin-4/13A and GATA-3 in gill and skin of salmonid fishes suggests that these tissues form Th2-skewed immune environments. *Mol. Immunol.* 48: 1360–1368.
- Takizawa, F., J. M. Dijkstra, P. Koterba, T. Korytár, H. Kock, B. Köllner, B. Jaureguiberry, T. Nakanishi, and U. Fischer. 2011. The expression of CD8 α discriminates distinct T cell subsets in teleost fish. *Dev. Comp. Immunol.* 35: 752–763.
- Koppang, E. O., C. M. Press, K. Rønningen, and Ø. Lie. 1998. Expression of Mhc class I mRNA in tissues from vaccinated and non-vaccinated Atlantic salmon (*Salmo salar*L.). *Fish Shellfish Immunol.* 8: 577–587.
- Jørgensen, S. M., S. Afanasyev, and A. Krasnov. 2008. Gene expression analyses in Atlantic salmon challenged with infectious salmon anaemia virus reveal differences between individuals with early, intermediate and late mortality. *BMC Genomics* 9: 179.
- Lukacs, M. F., H. Harstad, H. G. Bakke, M. Beetz-Sargent, L. McKinnel, K. P. Lubieniecki, B. F. Koop, and U. Grimholt. 2010. Comprehensive analysis of MHC class I genes from the U-, S-, and Z-lineages in Atlantic salmon. *BMC Genomics* 11: 154.
- Schatz, D. G., M. A. Oettinger, and D. Baltimore. 1989. The V(D)J recombination activating gene, RAG-1. *Cell* 59: 1035–1048.
- Oettinger, M. A., D. G. Schatz, C. Gorka, and D. Baltimore. 1990. RAG-1 and RAG-2, adjacent genes that synergistically activate V(D)J recombination. *Science* 248: 1517–1523.
- Snelgrove, R. J., A. Godlee, and T. Hussell. 2011. Airway immune homeostasis and implications for influenza-induced inflammation. *Trends Immunol.* 32: 328–334.

Corrections

Aas, I. B., L. Austbø, M. König, M. Syed, K. Falk, I. Hordvik, and E. O. Koppang. 2014. Transcriptional characterization of the T cell population within the salmonid interbranchial lymphoid tissue. *J. Immunol.* 193: 3463–3469.

In the version of this article initially published, labeling of the *x*-axis was missing from Fig. 4. The corrected Fig. 4 is shown below. The figure legend was correct as published and is shown below for reference.

The figure has been corrected in the online version of the article, which now differs from the print version as originally published.

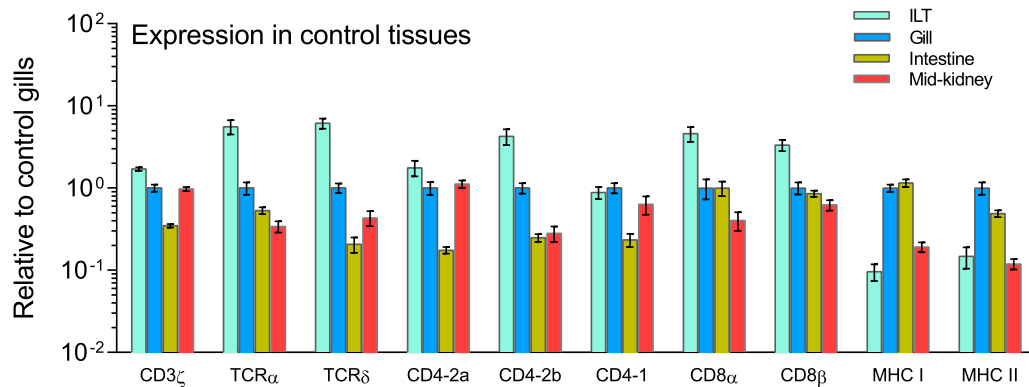


FIGURE 4. T cell–related transcript levels in the control group. Analysis of T cell–related markers show that all transcripts investigated were present in all organs examined. Transcript levels for the control group ($n = 8$) are displayed with mean \pm SEM. Transcript levels are normalized with EF1A_B and displayed relative to the mean of control gills.

www.jimmunol.org/cgi/doi/10.4049/jimmunol.1490047